Erika Hrehorova, Marian Rebros, Alexandra Pekarovicova, Bradley Bazuin, Amrith Ranganathan, Sean Garner, Gary Merz, John Tosch, and Robert Boudreau; *Gravure Printing of Conductive Inks on Glass Substrates for Applications in Printed Electronics*

JOURNAL OF DISPLAY TECHNOLOGY, Vol. 7; No. 6; pp. 318-324; June 2011

Gravure Printing of Conductive Inks on Glass Substrates for Applications in Printed Electronics

Erika Hrehorova, Marian Rebros, Alexandra Pekarovicova, Bradley Bazuin, Amrith Ranganathan, Sean Garner, *Member, IEEE*, Gary Merz, John Tosch, and Robert Boudreau

(Invited Paper)

***Abstract*—In graphics, gravure printing is the preferred method for printing high quality, fine dimension graphics using high-speed roll-to-roll or sheet fed presses. Gravure printing typically employs flexible and compressible substrates such as various papers and polymer films. In electronics, glass substrates are a common, if not preferred, substrate in many applications, particularly displays and photovoltaics. In combining printing with glass substrates, challenges exist in adapting contact-based printing methods such as gravure to the mechanical properties of the more rigid substrates. In this work, sheet-fed gravure printing has been successfully used to print silver-based conductive inks on glass substrates. Various features were designed and printed to evaluate conductive layers in terms of their printability and electrical performance. The independent variables include gravure cell dimensions, trace orientation with respect to printing direction and ink type. Results from this work provide an insight into the science of gravure printing on glass by correlating the independent variables to printed feature quality and electrical performance.**

***Index Terms*—Gravure printing, glass, printed electronics (PE), conductive ink, silver flakes, silver nanoparticles, electrical resistance.**

I. Introduction

PRINTED ELECTRONICS (PE) is a new rapidly advancing manufacturing field that is bringing together two traditional technologies, graphics printing and electronics manufacturing. Product areas that might benefit from PE manufacturing include radio-frequency identification (RFID), sensors, photovoltaics (solar cells), energy storage (batteries), etc. However, one of the biggest areas of interest for PE is various display technologies. The advantages of PE for these technologies represent the possibility to make large area displays at low cost and still achieve high quality products [1]. Through the combination of solution processable active materials and advanced printing technologies each functional layer can be potentially printed to construct a display on variety of substrates.

Manuscript received April 14, 2010; revised July 24, 2010; accepted July 27, 2010. Date of publication September 20, 2010; date of current version April 27, 2011.

E. Hrehorova, M. Rebros, A. Pekarovicova, B. Bazuin, and A. Ranganathan are with the Center for the Advancement of Printed Electronics, Western Michigan University, Kalamazoo, MI 49008 USA (e-mail: erika.hrehorova@wmich.edu; mrebros@wmich.edu; a.pekarovicova@wmich.edu; brad.bazuin@wmich.edu; amrith.ranganathan@wmich.edu).

S. Garner, G. Merz, J. Tosch, R. Boudreau are with the Corning Inc., Corning, NY 14831 USA (e-mail: GarnerSM@corning.com; MerzGE@corning.com; MerzGE@corning.com; ToschJE@corning.com; BoudreauRA@corning.com).

Digital Object Identifier 10.1109/JDT.2010.2065214

Yet, before printing can be fully adopted for display manufacturing, a few issues have to be addressed. Traditional printing technologies have to be improved to meet display manufacturing requirements which include high resolution, precise layer-to-layer registration and adopting substrates that have not been normally employed by printing industry.

For many years, gravure printing has been considered a process capable of producing the highest quality printed products. Outside the well-established graphic arts applications, gravure is gaining a lot of attention as a potential low-cost manufacturing method for various PE applications [2]–[8]. Some of the advantages of gravure printing that make it an attractive process for structuring layers for electronics include high resolution printing, the ability to print low viscosity inks, solvent resistance of the image carrier and long-run stability at high printing speeds. Moreover, gravure printing has the ability to deposit a very wide range of ink film thicknesses in one print unit, a feature that is a limitation in other printing processes such as flexography, inkjet and offset printing. It can also be used for a broad range of substrates with a wide range of ink formulations.

Gravure printing is mechanically simpler when compared to other printing processes. It has four basic components to each printing unit: an image carrier (engraved cylinder), ink fountain (inking pan), doctor blade, and impression roller (Fig. 1). The heart of a gravure press is the engraved cylinder, which carries the image design to be printed.

Renewed interest in gravure printing for manufacturing of PE is driving the improvements in the quality of cylinder engraving far beyond the requirements of graphic technology needs to satisfy a resolution of human eye. High quality engraving improvements, including resolution and registration, are crucial in the production of functional electronic components. Traditionally, in gravure printing, the image is broken down into individual cells. Fine text and lines are typically engraved as rows of discrete dots and thus ink spreading is essential in order to form continuous contours. Many improvements in the quality of engraving have been made by utilization of laser technologies, which offers much higher resolutions and smoother edge definition than is possible with traditional electromechanical engraving.

The majority of gravure substrates are flexible and can be printed in a web-fed or roll-to-roll process. For printed electronics, however, substrates with higher dimensional stability than paper or polymer film are of high interest to improve resolution, registration, and device performance. Glass has

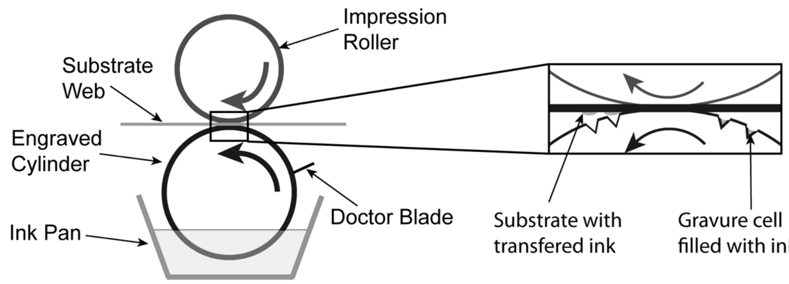

Fig. 1. Basic principle and arrangement of the components for gravure printing.

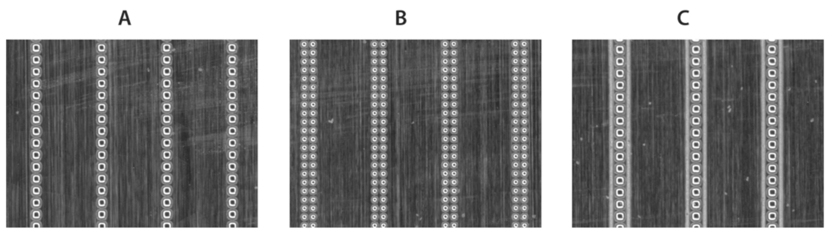

Fig. 2. Examples of engraving for traces with nominal width: (A) 100 μm; (B) 150 μm; and (C) 200 μm. (Images taken with ImageXpert Image Analysis System at 40× magnification.)

been used in the electronics industry for many years due to its several key characteristics: 1) very high thermo-mechanical stability; 2) high surface quality; 3) chemical resistance; and 4) excellent barrier to oxygen and moisture, which makes it a very attractive substrate for the highly sensitive materials typically used in organic PE.

Among printing processes, screen printing is probably the most often used to print electronic inks on rigid substrates, including glass. Other printing methods that can be used with rigid substrates are either non-contact, (e.g., inkjet printing [9] or aerosol printing [10]) or methods requiring only slight contact pressure for ink transfer (e.g., gravure offset printing [11] or pad printing [12]). Direct gravure printing requires higher impression pressure, and, therefore, the lower glass compressibility creates unique challenges for its use with gravure.

This paper evaluates glass as a potential substrate for high performance gravure printed electronics with the demonstration of silver-layer conductors.

II. Experimental Set-up

A. Gravure Cylinder Engraving and Printing

A gravure cylinder was designed and engraved to include a set of meander line resistors that were used for both printability evaluation and DC resistance testing. Test structure line (trace) widths were designed to range from 50 to 500 μm. In order to evaluate directionality effects of gravure printing, traces were designed at three different angles with respect to the print direction, namely 0°, 45°, and 90°. For the evaluation of printed gaps, a group of 500 μm wide lines with different spacing was included. The printed area had dimensions of 105 mm×300 mm, which fit three repeats of the design (a scanned image of the actual printed sample is shown in Fig. 13; actual dimensions of the scanned printed area are 100×105 mm which corresponds to one repeat).

The gravure cylinder was engraved by RotaDyne Decorative Technologies (Cincinnati, OH) using an indirect laser method. Indirect laser engraving involves laser ablation of a protective mask on a copper surface, followed by a chemical etching of the copper layer [13]. After etching, the cylinder was chromium plated and finished using traditional methods [14]. A typical shape of engraved cell resembles a squared cup. For this work, ,a target cell depth of 30 μm was used. Traces with widths of 50, 75 and 100 μm were composed of one row of engraved cells as shown in Fig. 2(A). Two rows of cells were used to form 150μm wide traces [Fig. 2(B)]. Traces with nominal width of 200 and 500 μm were engraved as a group of cells with a moat on the edges of the line [Fig. 2(C)].

Gravure printing was performed using a sheet-fed gravure proofer, Prüfbau Rotogravure Printability Tester (by Prüfbau, Germany). The main advantage of this tester is that it is capable of printing onto substrates with varying flexibility; hence it could be used for printing on relatively rigid glass substrates. Printing on glass is facilitated by using a flat and rigid carrier covered with an impression blanket (thickness of impression blanket 2.5 mm, Shore A hardness of 86) to support the substrate. The carrier was then manually fed between the back-up roller and rotating printing cylinder. The printing nip was created by the contact between substrate and cylinder and the rotation of the cylinder propelled the substrate through the nip transferring the ink from engraved cells onto the test substrate. A printing speed of 250 fpm (1.27 m/s) was used during the printing trial. The carrier with printed substrate was pushed to the carrier slider, collected, and the substrate was detached and dried as described in the next section.

B. Materials

Two silver-based conductive inks were used in this work, one containing silver flakes (PM-500 by Henkel Corp. with flake size < 3 μm) and the other containing silver nanoparticles (TEC-PR-020 by Inktec, Inc. with particle size 20–50 nm) as the conductive filler. Fig. 3 shows viscosity curves for the inks used as measured with an AR 2000 Advanced Rheometer (TA Instruments). It can be seen that the nanosilver ink had a

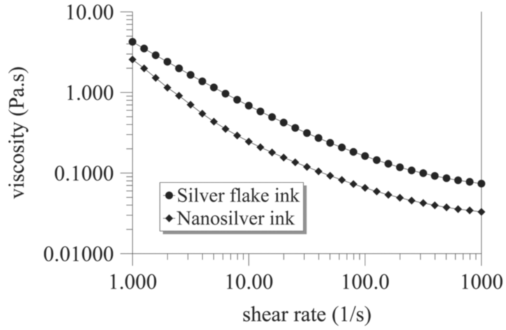

Fig. 3. Viscosity curves for conductive inks used in this work.

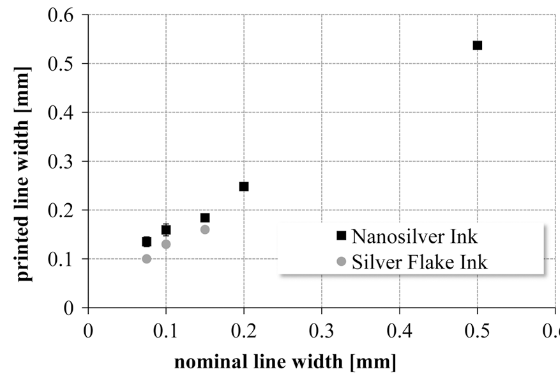

Fig. 4. Comparision of printed versus nominal line width in print direction for two conductive inks printed on glass substrate.

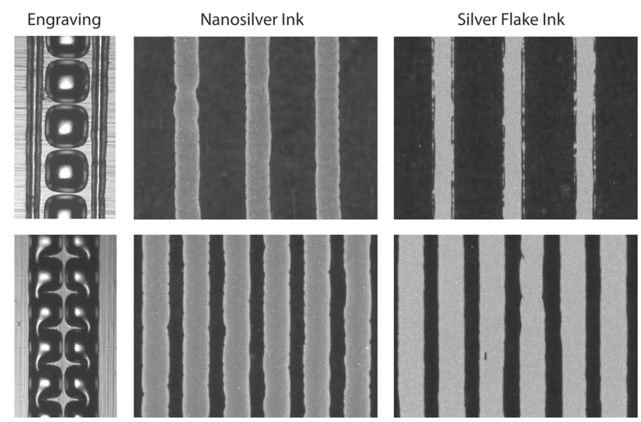

Fig. 5. Comparison of printability of 200 μm nominal line by using two different engraving approches.

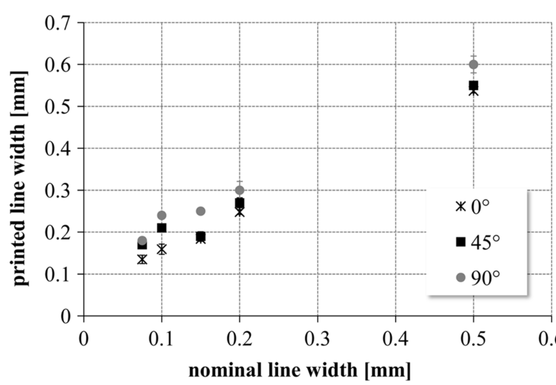

Fig. 6. Printed versus nominal line width for nanosilver ink printed on glass at three different angles to print direction.

lower viscosity than the silver flake ink over the whole range of measured shear rates. The main differences between the silver inks are particle size, particle shape, resin system and solids content. Unfortunately, there is very little information available about the composition of silver inks, which limits the user to only control the solids content. The solids content of silver inks was adjusted by adding appropriate solvents (PM-511 solution by Henkel Corporation for silver flake ink and isopropyl alcohol for nanosilver ink) based on previous studies with gravure printing of these silver inks. For printing trials, the solids content of silver flake and silver nanoparticle inks were around 80 wt% and 40 wt%, respectively. Printed inks were initially cured using a heat-gun for 1 min followed by post-curing treatment in a convection oven at 120 °C for 10 min.

Glass substrates were supplied by Corning Inc., Corning, NY. The glass substrates were 110 mm×310 mm and 0.7 mm thick. A representative UV curable acrylate coating (< 10 μm thick) was applied to the substrate surface to ensure ink adhesion. Prior to printing, the glass substrates were cleaned in subsequent baths of de-ionized water and isopropyl-alcohol and then dried. Atomic force microscope analysis of the coated surface after cleaning showed a Ra roughness value of about 1 nm. Surface energy of around 50 mN/m was calculated for the coated substrate based on contact angle measurements with methylene iodide and water.

C. Sample Evaluation

Quality of printed lines and gaps was evaluated using the ImageXpert Image Analysis System. Ink film thickness was measured by a vertical scanning interferometry (VSI) using a WYKO RST-Plus microscope. Electrical DC resistance measurements of printed glass samples were performed using the 2 point probe local measurement with the standard ohm-meter settings on the Keithley 2602 while sourcing a 1 mA current.

III. Results and Discussion

Printed conductive layers can fulfill various functions in PE devices, such as contact electrodes for transistors, capacitors and diodes or as interconnecting wires. Depending on the function of the conductive layers, they need to be highly conductive and very smooth with well-defined minimal line width and spacing to assure the desired electrical performance and quality of subsequent layers. In this work, line quality was evaluated in terms of ability to hold designed dimensions. DC resistance was measured as an indicator of printed feature performance.

A. Line and Gap Quality

A comparison of printed versus nominal (designed) line width for nanosilver and silver flake inks printed on glass substrates is shown in Fig. 4. These results were obtained from measurements of lines printed in parallel with print direction (0°). When comparing the inks used, it can be seen that the lines printed with nanosilver ink spread more than lines printed with silver flake ink. This is caused by the higher viscosity of

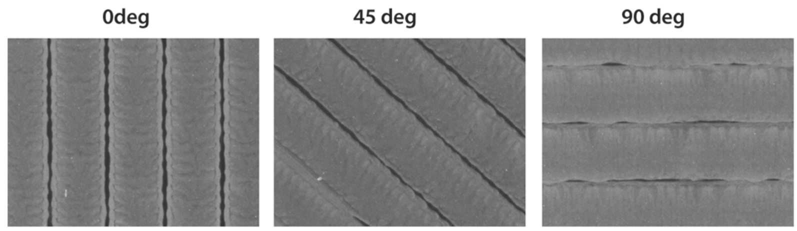

Fig. 7. Comparison of gap quality 50 μm nominal gap for nanosilver ink printed at three different angles to print direction.

silver flake ink as well as a higher solids content, which leads to faster ink setting and therefore less spreading. In Fig. 4, it can be seen that there are missing values for 200 and 500 μm nominal lines for silver flake ink. This is due to printability issues with silver flake ink for lines printed with an engraving moat as shown in Fig. 2(C). For these lines, the moat's narrow grooves surrounding gravure cells did not transfer a sufficient ink volume and resulted in a "satellite" line that was separated from the main line.

Fig. 5(A) shows the detail of engraving and a comparison of printed conductive line with nominal width of 200 μm for both conductive inks. In order to improve the printability of silver flake ink, a slightly different approach of creating a moat around the engraved cells was tried in a subsequent trial. The new engraving is shown in Fig. 5(B) together with corresponding line quality. Nanosilver ink was able to produce continuous lines with both types of engraving; however, the lines were different in width. Line widths for nanosilver ink were measured to be 248 ± 6 μm and 269 ± 7 μm for type A and type B engraving, respectively. For silver flake ink, engraving B resulted in very smooth line edge and line width of 263 ± 5 μm.

Fig. 6 shows the results for printed versus designed line width for nanosilver lines printed on glass substrates at three different angles to the print direction. There was a significant line width gain (increase in printed line width from designed line width) observed for all printed lines. It can be seen that lines printed at 90° are the widest followed by lines at 45°, and finally lines printed in parallel to the print direction (0°) are the narrowest. Similar effects were seen previously when printing silver traces on paper substrates [15]. Interestingly, the 100 μm nominal lines printed with similar or even higher line width than the nominal 150 μm line. This was caused by different gravure cell sizes that were used to print these lines, which is shown in Fig. 2(A) and (B). The use of two rows of smaller cells for the 150 μm nominal lines caused a lower amount of ink to be transferred and therefore less line spreading.

The narrowest line and gap designed for this work was 50μm wide. Unfortunately, the cell spacing was too large for ink drops to spread and create continuous and conductive lines. In the future, gravure cells should be spaced closer to each other to assure better printability and consequently measurable conductivity.

As for the gap quality, Fig. 7 compares the 50 μm nominal gap for nanosilver ink in three different angles to the print direction. It can be seen that the gap printed in print direction (0°) is clean, and it was measured to be 36 ± 8 μm. However, for 45° and 90° the ink spreads into the gap causing a short circuit.

B. Ink Film Thickness

Ink layer thickness was measured for lines printed with silver flake and nanosilver ink on glass substrates only parallel to the print direction (0°). Typical images that can be obtained with VSI are shown in Fig. 8. This shows 100 μm nominal line width for both nanosilver and silver flake ink printed on glass substrate. It can be seen that lines printed with silver flake ink have larger thickness, and they are also rougher than nanosilver ink printed lines.

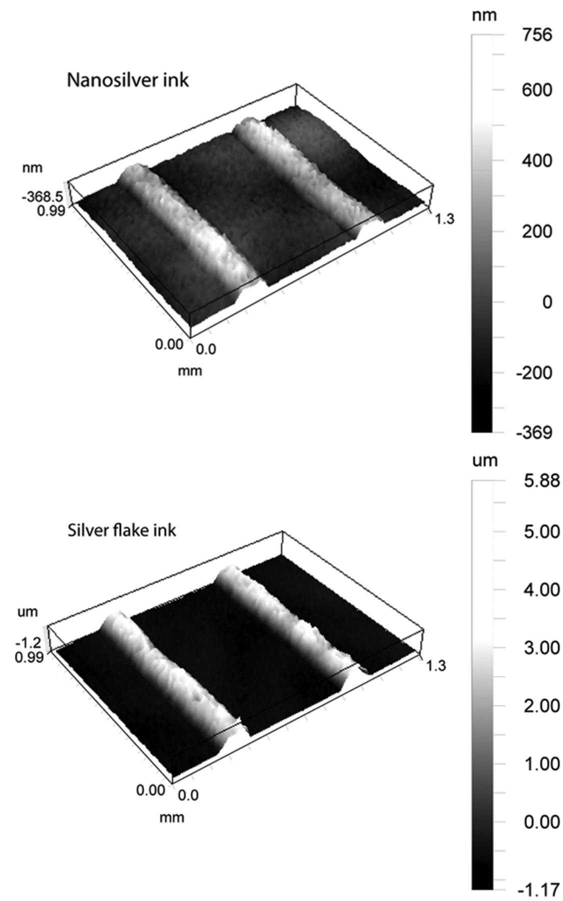

Fig. 8. 3D images of 100 μm nominal line printed with (top) nanosilver link and (bottom) silver flake ink on glass substrate (note the different vertical scale for the two images).

Fig. 9 shows the comparison of line thickness range for nanosilver and silver flake inks. It can be seen that silver flake ink produces significantly thicker lines than nanosilver ink. The thickness for nanosilver ink ranges from about 0.2 to 1μm, whereas lines printed with silver flake ink are as thick as 6 μm. These differences can be caused by much higher solid content in silver flake ink, larger particles and also higher ink viscosity. Generally, line thickness increases with increasing nominal line width, except for 100 and 150 μm lines. The 100 μm nominal line printed thicker than the 150 μm line for both

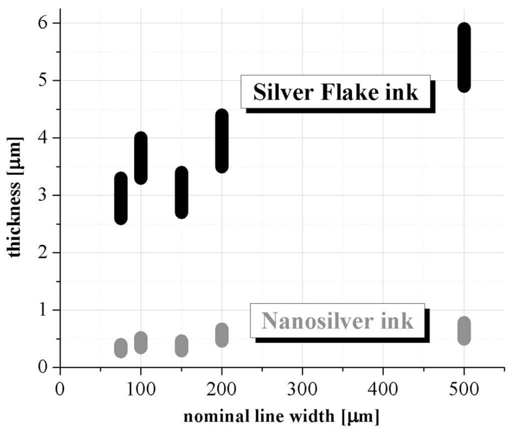

Fig. 9. comparison of line thickness range for different nominal line widths for the two conductive inks.

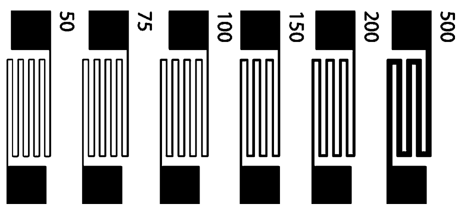

Fig. 10. Meander line resistors with different trace widths used for DC resistance measurements (not to scale).

inks. As previously discussed, there is a significant difference in the engraving of these two lines, which caused a 100 μm line to spread more and be thicker than a 150 μm line.

C. Electrical Properties

The DC resistance (R) of a rectangular line is based on the material resistivity, the length and cross-sectional area by

$$R = \rho * \frac{L}{A}. \quad (1)$$

Resistance measurements of the printed lines were performed on test structures with nominal line widths of 500, 200, 150, 100, 75, and 50 μm and lengths of 54, 75, 75, 96, 96, and 96 mm, respectively, designed as shown in Fig. 10. The resistance of each line was measured using a 2-terminal test and a Keithley 2602 Sourcemeter.

As the primary focus of the work is on the quality of printed lines on glass and the variance in line width and thickness, the average measured resistance values will be in terms of the material resistivity (ρ) and cross-sectional area (A) by scaling by the line lengths. Thus the reported values are in terms of resistance per millimeter

$$R/L = \rho/A. \quad (2)$$

As initial work on printing repeatable, predictable, high quality lines, it may also be noted that probe contact resistance or variance in the effective line lengths due to corners and measurement pad geometry have not been considered at this time.

Fig. 11 shows the resistance per millimeter values measured for structures with different line width for both tested inks printed in parallel to the print direction. It can be seen that silver flake ink has lower resistance than nanosilver ink for

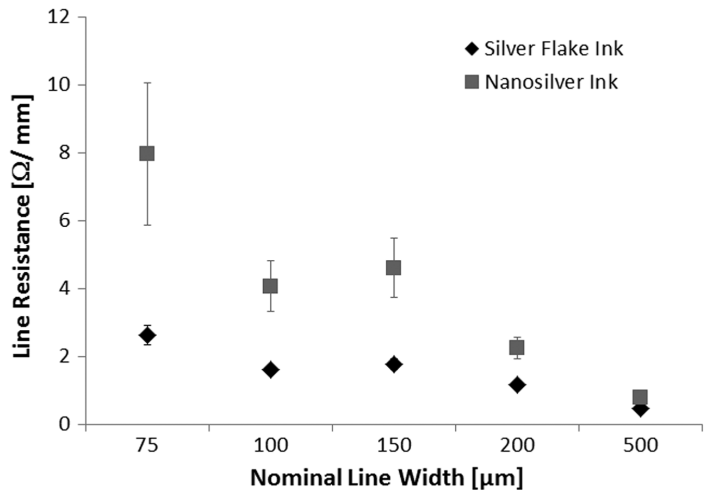

Fig. 11. DC resistance values for resistors with different nominal line widths for two counductive inks printed (lines printed in parallel to print direction, 0°).

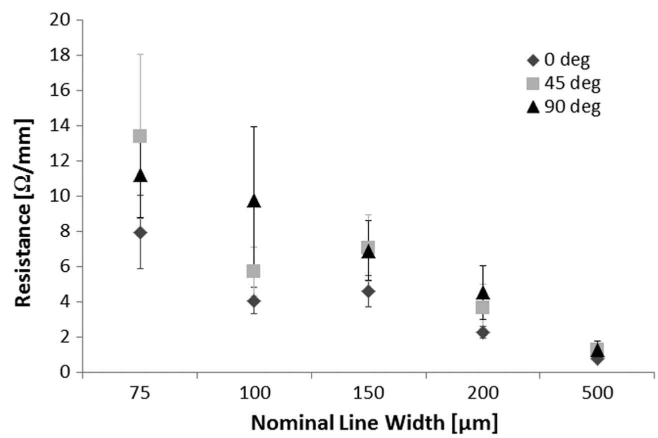

Fig. 12. DC resistance values for resistors with different nominal line widths for nanosilver ink printed at three different angles to print directin.

all measured line widths. As the nanosilver ink has a lower specified resistivity than the silver flake ink, this is somewhat counterintuitive. The result is directly attributable to the significant difference in ink film thickness providing the silver flake ink to have a greater cross-sectional area. The trend of increasing DC resistance with decreasing line width was observed for all nominal widths, except for the 150 and 100μm line resistors where 100 μm resistors typically produced comparable resistance values to 150 μm resistors. As the resistance is based on the cross-sectional area of the line, this is a further indication of the visual differences observed in printing the 100 and 150 μm lines. As discussed earlier, these differences are caused by different engraving of the cells that create corresponding features.

Fig. 12 shows resistance values for resistors printed with nanosilver ink at three different angles with respect to print direction. The resistances were found to be the lowest at 0° to print direction. Although the printing of lines at 90° angle to print direction exhibited more spreading and produced wider lines, the amount of the ink transferred from the gravure cells is assumed to be the same as for lines printed at 0°. The lines printed at 0° are narrower but more uniform than those printed

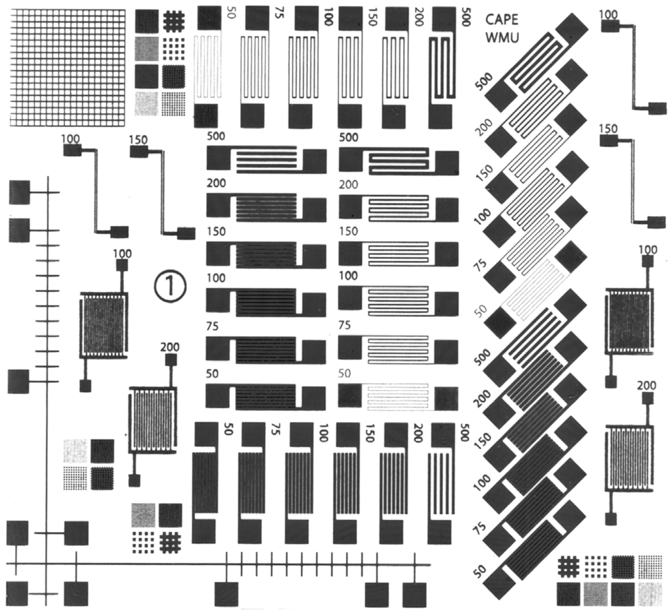

Fig. 13. A scanned image for one of three repeats for silver flake ink gravure printed on glass (actual dimensions of the scanned printed area are 100×105 mm).

at 90°, which led to better performance of 0° lines. Also as the nominal line width increases, resistance values for all print direction were more consistent, providing a smaller standard deviation of the measurement.

IV. Conclusion

This work demonstrated gravure printing of conductive traces on glass substrates for applications in printed electronics. Two different conductive inks, containing either micro-sized silver flakes or spherical nanoparticles, were used. The differences in ink characteristics lead to different printability and electrical performance for the two inks. It was shown that the engraving specifications and line orientation with respect to printing direction play an important role in the quality of printed conductive traces. This work demonstrates how to improve line printability by proper adjustments to the engraving.

The results of this work indicate the initial design and process trade-offs that exist when targeting high-performance gravure printed electronic devices on glass substrates. Optimization of processes to produce high resolution and high registration device structures is required to fully utilize the thermal capability, hermiticity, surface quality, and dimensional stability of glass substrates for printed electronics.

References

[1] D. Gamota, P. Brazis, L. Kalyanasunadaram, and J. Zhang, *Printed Organic and Molecular Electronics*. Boston: Kluwer Academic, 2004.

[2] M. Tuomikoski *et al.*, "Manufacturing of polymer light-emitting device structures," in *Proc SPIE—Int. Soc. Opt. Eng.*, Strasbourg, France, Apr. 3–6, 2006, art. no. 619204.

[3] J. Puetz and M. A. Aegerter, "Direct gravure printing of indium tin oxide nanoparticles patterns on polymer foils," *Thin Solid Films*, vol. 516, pp. 4495–4501, 2008.

[4] J. M. Ding, A. F. Vornbrock, C. Ting, and V. Subramanian, "Patternable polymer bulk heterojunction photovoltaic cells on plastic by rotogravure printing," *Solar Energy Mater. Solar Cells*, vol. 93, pp. 459–464, 2009.

[5] M. Rebros, E. Hrehorova, B. J. Bazuin, M. K. Joyce, P. D. Fleming, and A. Pekarovicova, "Rotogravure printed UHF RFID antennae directly on packaging materials," in *Proc TAGA 60th Annu. Tech. Conf.*, San Francisco, CA, Mar. 16–19, 2008.

[6] E. Hrehorova, M. Rebros, A. Pekarovicova, and P. D. Fleming, "Suitability of gravure printing for high volume fabrication of electronics," in *Proc. IS&T Conf. on Digital Fabrication*, Pittsburgh, PA, Sept. 6–11, 2008, pp. 260–264.

[7] E. Hrehorova, A. Pekarovicova, V. N. Bliznyuk, and P. D. Fleming, "Polymeric materials for printed electronics and their interactions with paper substrates," in *Proc IS&T Digital Fabrication*, Anchorage, AK, Sep. 16–20, 2007, pp. 928–932.

[8] A. F. Vornbrock, J. M. Ding, D. Sung, H. Y. Tseng, and V. Subramanian, "Printing and scaling of metallic traces and capacitors using a laboratory-scale rotogravure press," in *Proc. 2009 Flexible Electron. & Displays Conf.*, Pheonix, AZ, Feb. 2–4, 2009.

[9] Y. Liu and T. Cui, "Polymer-based rectifiying diodes on a glass substrate fabricated by ink-jet printing," *Macromolecular Rapid Commun.*, vol. 26, pp. 289–292, 2005.

[10] M. O'Reilly, "Aerosol jet direct write solutions for photovoltaic and other commercial markets," presented at the IDTechEx Conf. on Printed Electron. USA 2009, San Jose, CA, Dec. 1–4, 2009.

[11] J. Hagberg, M. Pudas, S. Leppavouri, K. Elsey, and A. Logan, "Gravure offset printing development for fine line thick film circuits," *Microelectron. Int.*, vol. 18, pp. 32–35, 2001.

[12] F. C. Krebs, "Pad printing as a film forming technique for polymer solar cells," *Solar Energy Mater. and Solar Cells*, vol. 93, no. 4, pp. 484–490, 2009.

[13] G. Henning, K. H. Selbmann, and A. Brocklet, "Laser engraving in gravure industry," in *Proc SPIE: Workshop on Laser Appl. in Eur.*, 2006, p. 6157, 61570C.

[14] K. Gillett *et al., Gravure—Process and Technology*, 2nd ed. Rochester, NY: GAA and GEF, 2003, pp. 231–235.

[15] E. Hrehorova, A. Pekarovicova, and P. D. Fleming, "Evaluation of gravure printing for printed electronics," in *Proc TAGA 60th Annu. Tech. Conf.*, San Francisco, CA, Mar. 16–19, 2008, pp. 324–336.

Erika Hrehorova received the B.Sc. degree in chemical engineering and M.S. degree in polymer materials from the Slovak University of Technology, Bratislava, Slovakia, in 2000 and 2002, respectively, and the M.S. and Ph.D. degrees in paper and imaging science and engineering. from the Western Michigan University, Kalamazoo, MI, in 2005 and 2007, respectively.

She is currently an Assistant Professor in the Department of Paper Engineering, Chemical Engineering and Imaging and a member of the Center for the Advancement of Printed Electronics at Western Michigan University, Kalamazoo, MI. While at PCI, she had worked as a teaching assistant and instructor for multiple undergraduate courses regarding gravure printing, printing ink, paper engineering, imaging, etc. During her doctoral studies she has focused on suitability of conventional printing technologies, such as gravure or flexographic printing, in electronics manufacture. Presently, she continues to work in the field of printed electronics and her main research interests are focused on formulation and characterization of functional inks as well as optimization of process parameters for improved quality and performance of printed electronic components.

Alexandra Pekarovicova, photograph and biography not available at time of publication.

Bradley Bazuin, photograph and biography not available at time of publication.

Amrith Ranganathan, photograph and biography not available at time of publication.

Sean Garner (S'95–M'98) received the B.Eng. degree in engineering physics (applied laser and optics) from Stevens Institute of Technology, Newark, NJ, in 1993, and the Ph.D. degree in electrical engineering (electrophysics) from the University of Southern California, Los Angeles, in 1998.

Since 1998, he has been working in the area of materials processing and devices at the Science and Technology Center, Corning Inc., Corning, NY. He has co-authored over 80 journal articles and conference presentations, and he is currently leading efforts at Corning investigating flexible device substrates.

Dr. Garner is a founding co-chairman for the Rochester IEEE-LEOS Chapter, and currently chairman of the IEEE Photonics Society (formerly, IEEE Lasers and Electro-Optics) Displays committee.

Gary Merz, photograph and biography not available at time of publication.

John Tosch, photograph and biography not available at time of publication.

Robert Boudreau, photograph and biography not available at time of publication.